Electrochemical performance of activated screen printed carbon electrodes for hydrogen peroxide and phenol derivatives sensing

M.I. González-Sánchez[a], B. Gómez-Monedero[a], J. Agrisuelas[b], J. Iniesta[c] and E. Valero[a*]

[a]Department of Physical Chemistry, Higher Technical School of Industrial Engineering, University of Castilla-La Mancha, Campus Universitario s/n, 02071, Albacete, Spain. MIsabel.Gonzalez@uclm.es; Beatriz.Gomez@uclm.es; Edelmira.Valero@uclm.es

[b]Department of Physical Chemistry, Faculty of Chemistry, University of Valencia, C/ Dr. Moliner 50, 46100 Burjassot, Valencia, Spain. Jeronimo.Agrisuelas@uv.es

[c]Department of Physical Chemistry and Institute of Electrochemistry, University of Alicante, 03690, San Vicente del Raspeig, Alicante, Spain. Jesus.Iniesta@ua.es

*Address correspondence to Edelmira Valero: Edelmira.valero@uclm.es.

Declarations of interest: none

Abstract

Screen-printed carbon electrodes (SPCEs) are widely used for the electroanalysis of a plethora of organic and inorganic compounds. These devices offer unique properties to address electroanalytical chemistry challenges and can successfully compete in numerous aspects with conventional carbon-based electrodes. However, heterogeneous kinetics on SPCEs surfaces is comparatively sluggish, which is why the electrochemical activation of inks is sometimes required to improve electron transfer rates and to enhance sensing performance. In this work, SPCEs were subjected to different electrochemical activation methods and the response to H_2O_2 electroanalysis was used as a testing probe. Changes in topology, surface chemistry and electrochemical behavior to H_2O_2 oxidation were performed by SEM, XPS, cyclic voltammetry, chronoamperometry and electrochemical impedance spectroscopy. The combination of electrochemical activation methods using H_2SO_4 and H_2O_2 proved particularly effective. A reduction in charge transfer resistance, together with functionalization with some carbon-oxygen groups on carbon ink surfaces, were likely responsible for such electrochemical improvement. The use of a two-step protocol with 0.5 M H_2SO_4 and 10 mM H_2O_2 under potential cycling conditions was the most effective activation procedure investigated herein, and gave rise to 518-fold higher sensitivity than that obtained for the untreated SPCEs upon H_2O_2 electrooxidation. The electrochemical behavior of acetaminophen, hydroquinone and dopamine is also shown, as a proof of concept upon the optimum activated SPCEs.

KEYWORDS: Screen-printed carbon electrodes, hydrogen peroxide, sulfuric acid, electrochemical activation, sensor, phenolic compounds.

1. Introduction

Screen-printed electrodes (SPEs) are single-use electrochemical devices based on conductive inks that arose from the need to create suitable reproducible, stable and disposable tools for low-cost mass production [1]. They allowed the replacement of traditional beaker-type electrochemical cells with easy-to-use sensors that support the analysis of microvolumes of samples [2]. For all these reasons, SPEs have attracted considerable attention in recent years, with a plethora of applications in not only fundamental research [3,4], and clinical [5], environmental [2] and food analyses [6-8], but also in teaching [9, 10].

The working electrodes in SPEs are made of conductive inks based on platinum, gold, silver or carbon materials that also contain binding pastes, such as resins or cellulose acetate, solvents such as terpineol, ethylene glycol or cyclohexanone, and additives that provide functional characteristics [11]. Among SPEs, screen-printed carbon electrodes (SPCEs) are the most widely used for sensing applications because they are relatively inexpensive and lead to low background currents and a wide potential window. Such carbon inks are generally composed of graphite particles, a polymeric binder and other additives. Slow electrode kinetic constants can appear in SPCEs and they are sometimes electrochemically activated to enhance their electrochemical performance [12, 13]. Pre-treatment of carbon-based electrodes can have an outstanding effect on the amelioration of electron transfer rates on a large number of compounds in solution [14, 15]. The activation cited in the bibliography typically involves holding the electrode at a constant potential for a short period of time [12, 13, 16], potential cycling to extreme potentials [17, 18], heat treatment [19], ultrasonic polishing [20], oxygen plasma treatment [21] or mechanical activation [22, 23]. Improved electroanalytical outputs after electrode activation may be attributed to an increment in the surface's hydrophilicity [14, 24], the increased quantity of carbon-oxygen functional groups on surfaces [25, 26], augmented surface roughness [27] and/or the removal of the organic ink constituents or contaminants introduced into the printing stage [14].

Recently, our group reported the generation of highly activated SPCEs through electrochemical treatment using H_2O_2 [28] that consisted of repetitive cyclic voltammetry in a phosphate-buffered solution of 10 mM H_2O_2 with remarkably improved electroanalytical output for H_2O_2 sensing compared to that of untreated SPCEs (nSPCEs). Both the introduction of new carbon-oxygen groups to carbon ink,

and the reduction in electron charge transfer resistance, were demonstrated as being the main responsible factors for improved electroanalytical output. Encouraged by the above results, the present study aimed to first compare different electrochemical activation methodologies described in the literature (*vide infra*), and then to explore the combination of already established activation methods with the best electrochemical performance tested herein for the electroanalytical sensing of H_2O_2. A comparison of electroanalytical outputs was made by a chronoamperometric analysis of the electrochemical oxidation of H_2O_2 given the key role played by this compound in pharmaceutical, clinical, environmental, mining, textile and food manufacturing applications [29, 30]. Moreover, H_2O_2 electrochemical performance using activated SPCEs (aSPCEs) was correlated with changes in topology, roughness factor, surface chemistry, electrochemical response of redox probes sensitive to surface functionalization and charge transfer resistance. Finally, in order to confirm the unrestricted applicability of aSPCEs, the best activation methodology was proven to explore the electrochemical behavior of model electroactive species, such as acetaminophen, hydroquinone and dopamine, as a proof of concept given their importance in clinical, pharmaceutical and environmental applications [31-33].

2. Material and Methods

2.1. Chemical and solutions

Acetaminophen, ammonium iron (II) sulfate hexahydrate, dopamine hydrochloride, hexaammineruthenium (III) chloride, hydrogen peroxide, hydroquinone, sodium phosphate monobasic and sodium ferrocyanide decahydrate were purchased from Sigma-Aldrich (Spain). Perchloric acid and sodium hydroxide came from Merck. Sulfuric acid and sodium phosphate dibasic were acquired from Panreac, and potassium chloride from Scharlau. All the reagents were purchased at their highest available purity and used without further purification. Solutions were prepared with deionized water (resistivity ≈ 18.2 MΩ·cm at 25°C) (Millipore, Watford, UK) and were freshly prepared every day. Sodium phosphate-buffered solution (PB) 0.1 M (pH 7) was used as the supporting electrolyte.

2.2. Electrochemical measurements

Electrochemical experiments were performed using a computer-controlled potentiostat AUTOLAB PGSTAT128N with an electrochemical impedance spectroscopy (EIS) analyzer (Eco Chemie B.V., The Netherlands) using the NOVA 2.0 software. The electrochemical measurements were taken on disposable SPEs (Dropsens), which consist of carbon (SPCE, DRP-150) or platinum (SPPtE, DRP-550) working electrodes (geometric area: 12.6 mm^2), a platinum counter electrode and a pseudo-silver reference electrode. Unless otherwise indicated, all the potentials in this paper refer to this electrode.

Table 1 compiles the experimental conditions of all the activation protocols used herein. Electrochemical pretreatments were performed by immersing the SPCE electrode into the corresponding solution under aerated conditions. All the measurements were taken at room temperature. After activation, electrodes were rinsed thoroughly with deionized water and air-dried.

Table 1. Experimental conditions used in each activation protocol. The first column shows an abbreviation assigned to each activation method for better clarity.

Protocol name	Concentration	Treatment	Reference
nSPCE	-	No treatment	-
1Na	0.1 M NaOH	Application of -1.2 V for 20 s	[13]
2P	0.05 M PB (pH 7, 0.05 M KCl)	Application of +1.7 V for 60 s	[16]
3S	0.05 M H_2SO_4	1 voltammetric cycle between -2.5 and +2.5 V at 100 mVs^{-1}	[18]
4H	0.01M H_2O_2 (in 0.1 M PB pH 7)	25 consecutive voltammetric cycles between +1 and -0.7V at 10 mVs^{-1}	[28]
5S	0.5 M H_2SO_4	10 consecutive voltammetric cycles between +2 and -0.3 V at 100 mVs^{-1}	[17]
6SH	0.05 M H_2SO_4 and 0.01 M H_2O_2	Activation 3S, followed by 4H	This work
7SH	0.5 M H_2SO_4 and 0.01 M H_2O_2	Activation 5S, followed by 4H	This work

The electroactive areas of SPEs were calculated by performing cyclic voltammetry at different scan rates using 10 mM $[Ru(NH_3)_6]Cl_3$ in 0.1 M KCl aqueous solutions previously bubbled with nitrogen gas [34, 35]. The Randles-Sevcik equation was used for this purpose.

The electroanalysis of H_2O_2 was performed in PB (0.1 M, pH 7) with constant stirring at a potential of +0.7 V and 25 ºC by immersing the electrode into a beaker with a 10 ml volume. To further clarify, it is worth noting that, in some cases, besides H_2O_2 being the reagent used to activate the electrode surface, it was also the analyte to be quantified. The analytical measurement of the micromolar amounts of H_2O_2 by chronoamperometry at +0.7 V did not activate the electrode.

EIS was carried out at 0.22 V in 10 mM $Na_4Fe(CN)_6$ and 0.1 M KCl. SPCEs were polarized for 30s. Then a sinusoidal amplitude potential perturbation (5 mV *rms*) was imposed between 65 kHz and 10 mHz, with five points per decade. The experimental data were fitted to a modified Randles equivalent circuit by the EIS Spectrum Analyzer v.1 (http://www.abc.chemistry.bsu.by/vi/analyser/) [36].

2.3. Physico-chemical characterization of SPCEs

Field emission SEM images were acquired in a Jeol 6490LV electron microscope equipped with detectors for secondary and backscattered electrons, which operated at an acceleration voltage of 30 kV.

The X-ray photoelectronic spectroscopy (XPS) experiments were recorded by a K-Alpha Thermo Scientific spectrometer using Al-Kα (1486.6 eV) radiation, monochromatized by a twin crystal monochromator to yield a focused X-ray spot with a diameter of 400 μm mean radius. The alpha hemispherical analyzer was used as an electron energy analyzer that operates in the fixed analyzer transmission mode, with survey scan pass energy of 200 eV and 40 eV narrow scans. The angle between the X-ray source and the analyzer (magic angle) was 54.7°. Processing of the XPS spectra was performed using the Avantage software, with energy values referenced to the C 1s peak of adventitious carbon located at 284.6 eV, and a Shirley-type background.

3. Results and Discussion

3.1. Activation of SPCEs by different methods

The activation pretreatment proposed in our previous work [28] was taken as a starting point to compare different reported activation methods in either the literature or by combining already established ones (Table 1). The effectiveness of pretreatments in activating SPCEs was evaluated by the electroanalysis of H_2O_2. Figure 1 shows the linear sweep voltammetries (LSVs) of the untreated SPCEs (nSPCEs) and the electrodes pretreated by the methods shown in Table 1 (aSPCEs). In all cases, and as a result of the pretreatments, some changes in carbon inks happened, which promoted H_2O_2 oxidation at lower potentials. For the 4H and 7SH treatments, the lowest potential values were obtained (the oxidation wave shifted from ~1.2 V in nSPCEs to ~0.7 V in these pretreated SPCEs), but the 5S electrochemical pretreatment also provided an ill-anodic wave that came close to that obtained for 4H and 7SH. Therefore, amperometric measurements of H_2O_2 were performed at 0.7 V for further experiments.

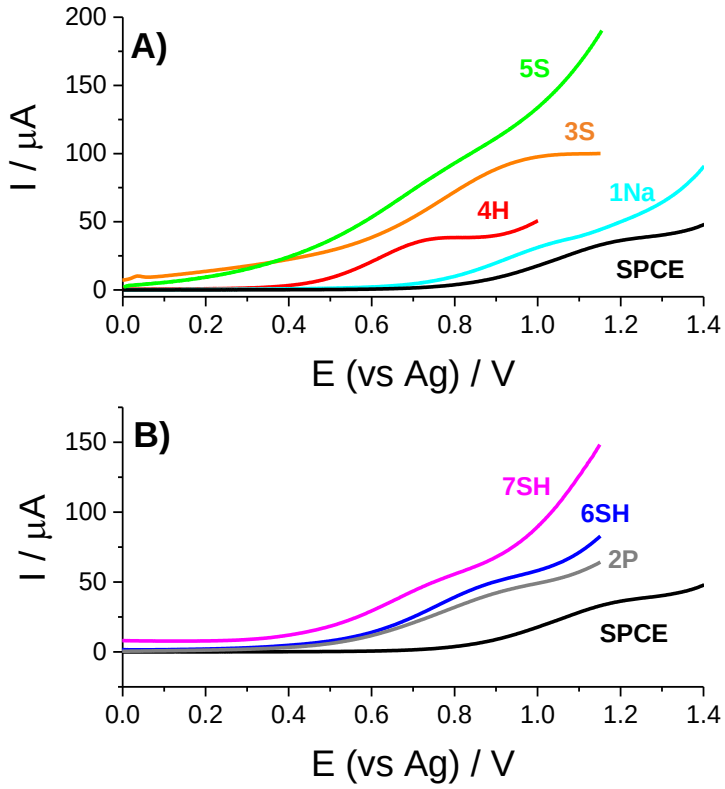

Figure 1. LSVs of 1 mM H_2O_2 using an nSPCE and aSPCEs generated by the different methods depicted in Table 1. Measurements were taken in PB (pH 7) at 50 mVs^{-1}.

Figure 2A shows the chronoamperometric response of the SPCEs subjected to the different one-step electrochemical pretreatments (1Na, 2P, 3S, 4H and 5S) to H_2O_2 electrooxidation. All the pretreatments led to an enhanced electrochemical response compared to the nSPCE (the corresponding analytical parameters are shown in Table 2), except for the treatment with NaOH, which did not significantly modify the output for H_2O_2 oxidation under our experimental conditions. The most sensitive response was obtained for the activated electrode with 0.5 M H_2SO_4 (named 5S).

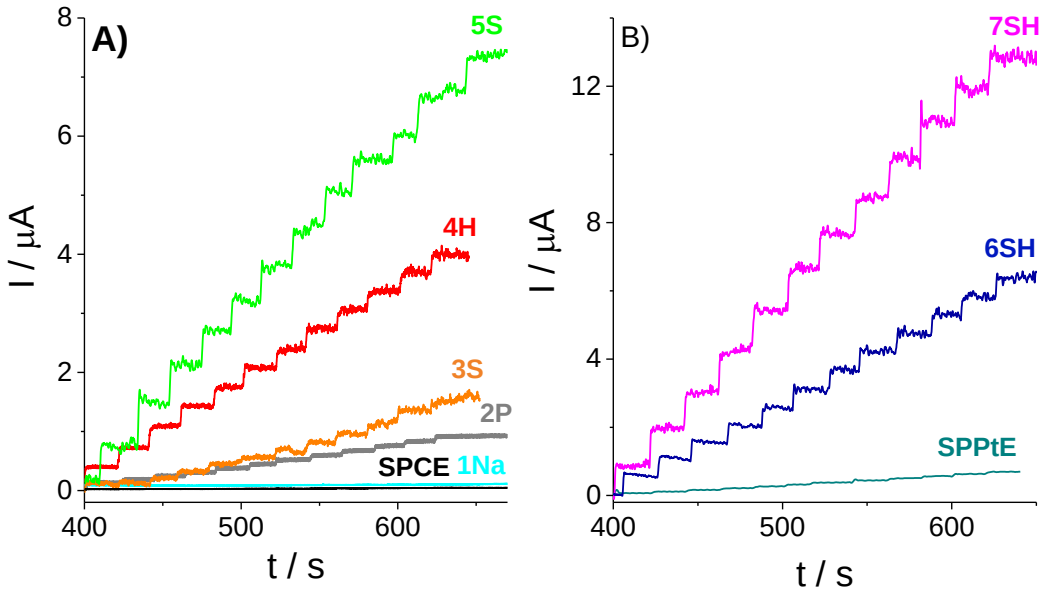

Figure 2. Chronoamperometric response at 0.7 V (vs. Ag) to the 10 µM H_2O_2 additions under steady-state conditions using an nSPCE and different aSPCEs generated by following the methods summarized in Table 1 and an SPPtE.

To further improve the activation processes, we checked some activation protocols consisting in two electrochemical steps (Figure 2B, activations 6SH and 7SH). The process consisted of a combination between pretreatment 3S or 5S and protocol 4H in two separate electrochemical steps; *viz.* the first one using H_2SO_4 and the second employing H_2O_2, which led to two different activation protocols (6SH and 7SH, respectively, Table 1). A change in the order of stages (i.e. first H_2O_2 and then H_2SO_4), or the simultaneous presence of H_2O_2 and H_2SO_4 in the same solution, revealed lower electroanalytical output to H_2O_2 (Figure 1S, Supplementary Material). These combined protocols yielded a very meaningful improvement of the current output to H_2O_2

oxidation compared to nSPCEs. Pretreatment 6SH achieved a sensitivity of ca. 245 times compared to that obtained for the untreated SPCEs, whereas 7SH improved 518-fold the sensitivity of nSPCEs to H_2O_2 (Table 2). In addition, the two-step methods 6SH and 7SH also showed significantly improved sensitivity compared to their corresponding one-step methods 3S and 5S, respectively. Thus the sensitivity attained with treatment 6SH was nearly 5-fold higher than that obtained with protocol 3S, while sensitivity attained with treatment 7SH was nearly twice that obtained with protocol 5S. However, the one-step treatment 5S showed a slightly higher sensitivity than the two-step treatment 6SH because, in the latter case, the sulfuric acid concentration used in the first step of the pretreatment was lower. In terms of LOD values, both the one-step 4H and the two-step 6SH and 7SH protocols provided the best outcomes (Table 2). Interestingly, the two-step treatments 6SH and 7SH gave lower LOD values than the one-step protocols 3S and 5S.

Table 2. Sensitivity and LOD values for the electroanalysis of H_2O_2 using aSPCEs subjected to the different activation treatments.

Treatment	**Sensitivity ($nA\mu M^{-1}cm^{-2}$)**	**LOD* (μM)**
None	1.7 ± 0.1	82.6
1Na	1.9 ± 0.2	64.1
2P	56.4 ± 0.9	16.7
3S	88.9 ± 3.2	13.9
4H	261.9 ± 1.4	2.2
5S	464.9 ± 5.6	10.8
6SH	419.8 ± 3.7	2.3
7SH	880.9 ± 9.2	2.7
SPPtE**	44.0 ± 1.0	1.9

*LOD was calculated based on $3\sigma/S$, where σ is the standard deviation of the blank and S is sensitivity. For all the experiments, the employed linear concentration

range was 10-120 μM. **Data corresponding to an SPPtE (no pretreatment) are included for comparison purposes.

Therefore, the best pretreatment for the amperometric electroanalysis of H_2O_2 with SPCEs was 7SH. The linear voltammetries in the presence of 1 mM H_2O_2 solution at different scan rates were performed using an nSPCE and an aSPCE treated by this method (Figure 2S, Supplementary Material). In both cases, diffusional behavior was found as the plot of current intensity *vs.* the square root of the scan rate gave a straight line (insets in Figure 2S, Supplementary Material).

Almost all the methods tested herein, except for 1Na, provided higher sensitivities for H_2O_2 electrooxidation than that based on the platinum screen-printed electrodes (SPPtEs) (Table 2 and Figure 2B). The improvement in the signal compared to SPPtEs is of key importance because the electrodes based on metallic Pt are widely used for the electroanalytical sensing of H_2O_2 [37, 38]. The possible substitution of these platinum electrodes for activated carbon electrodes could be important if we consider the cheapness of carbon inks compared to precious metal inks. Additionally, these sensitivities are higher than that obtained with other modified screen-printed carbon electrodes, such as iron-tetrasulfophthalocyanine-graphene-nafion modified SPCEs, although in this case the authors achieved better LOD for H_2O_2 at a lower potential [39].

3.2. Characterization of the electrode surface of aSPCEs

The improvement in sensitivity was expected to be related to changes in electrodes' surface. Electroactive areas, and the corresponding calculated percentages of the electroactive areas and roughness factors of the different electrodes, are shown in Table 1S (Supplementary Material). The electrodes activated using sulfuric acid (both the 1- and 2-step pretreatments, 3S, 5S, 6SH, 7SH) showed higher percentages of electroactive area (59.2-63.4%) and roughness factor (129.3-138.5%). Therefore in these electrodes, the increase in the electroactive area and roughness in relation to nSPCEs may offer a meaningful contribution to the activation of SPCEs. However in the other treatments (1Na, 2P and 4H), the electroactive area hardly changed, apart from showing lower percentages of electroactive area and roughness factors close to 100%. This finding indicates that other processes, such as the introduction of oxygenated functional groups (*vide infra*), could be involved in the activation of SPCEs. These

results agree with the electrochemical response to redox probe $Ru(NH_3)_6^{3+/2+}$ and the SEM analysis (Figures 3S and 4S, respectively, Supplementary Material). Redox probe $Ru(NH_3)_6^{3+/2+}$is an outer-sphere electron transfer that is insensitive to the C/O ratio groups and is affected only by changes in the electroactive area [22]. In general, no significant differences were observed between the cyclic voltammetries in Figure 3S (Supplementary Material), except for 5S, 6SH and 7SH pretreatments, which showed slightly higher intensity peaks and a greater capacitive current (see also Figure 4). In addition, the SEM analysis of the different aSPCEs (Figure 4S, Supplementary Material) revealed barely noticeable changes in the surface topology for the one-step treatments, but more porous surfaces for the electrodes treated by 6SH and 7SH.

EIS was used to monitor the electrode|solution interface changes of all the pretreated electrodes (Figure 3). Typical Nyquist plots were obtained for redox probe $Na_4Fe(CN)_6$. Therefore, a modified Randles circuit model was used to extract accurate information about the circuit elements (inset in Figure 3B). The equivalent circuit consists of an uncompensated resistance of the electrochemical cell (R_u), a charge transfer resistance at the electrode|solution interface (R_{ct}), and a constant phase element to characterize the double layer capacitance (CPE). To obtain the best fittings from the experimental data and the diffusion process of the redox probe, a Warburg element (W) was introduced into the circuit. Table 3 shows the values of the equivalent circuit elements obtained by fitting the experimental results for the Nyquist plots in Figure 3.

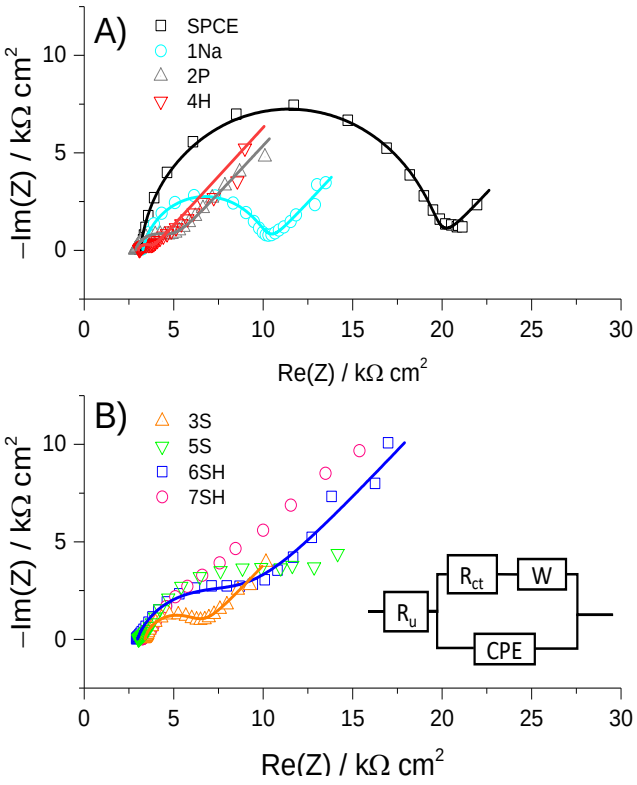

Figure 3. Nyquist plots for the different SPCEs. EIS were recorded at 0.22 V in 10 mM $Na_4Fe(CN)_6$ (in 0.1 M KCl). The inset in (B) shows the equivalent circuit used.

Table 3. Values of the equivalent circuit elements obtained by fitting the experimental results for the Nyquist plots shown in Figure 3.

Pretreatment	**R_u**	**R_{ct}**	**W**	**CPE**	**n**
	Ω cm^2	Ω cm^2	Ω cm^2 s$^{-1/2}$	μF cm^{-2}	
none	47.5	249.0	29.0	14.9	0.93
1Na	49.5	103.2	35.5	29.2	0.87
2P	43.6	29.0	68.7	183.0	0.82
3S	51.3	45.2	35.3	356.0	0.82
4H	45.6	11.1	60.6	80.2	0.80
5S	-	-	-	-	-

6SH	45.0	88.6	95.6	383.0	0.77
7SH	-	-	-	-	-

With these data, we observed that CPE and R_{ct} were the most sensitive elements to the activation treatments. The arcs or semicircles at relatively high frequencies in the Nyquist plots are related to R_{ct} at the electrode|solution interface. In general, any activation pretreatment of SPCEs reduced R_{ct}. In particular, pretreatment 4H significantly improved the electrical conductivity of aSPCEs (11.1 Ω cm^2) compared to nSPCEs (249.0 Ω cm^2). The higher R_{ct} of nSPCEs was due to the much lower conductivity properties of the carbonaceous ink. The depressed semicircles in the Nyquist plots are attributed to the presence of non-ideal double layer capacitances (CPE). In general, CPE increased (Table 3) as the roughness of electrodes incremented (Table 1S). A similar tendency was observed for exponent *n* of CPE, which moved away from ideality in the untreated SPCE (*n* close to 1 is characteristic of smooth surfaces [38, 40]) to *n* close to 0.77 in 6SH (modified aSPCE with one of the largest electroactive areas). For the aSPCEs activated by 5S and 7SH, the standard Randles equivalent circuit could not explain the impedance spectra, which was probably due to the increment in the electroactive area and roughness achieved after treatment (Table 1S). The most concentrated H_2SO_4 solution used in these activation processes considerably changed the surface, which could have caused the significant increment in the double layer capacity (*vide infra*, Figure 4) with the consequent masking of the diffusional branch at lower frequencies.

To gain further insight, electrodes were immersed in a solution containing $(NH_4)_2(FeSO_4)_2$ and cyclic voltammetries were performed (Figure 4); redox couple Fe^{2+}/Fe^{3+} is useful for predicting the existence of some functional groups as it is very sensitive to certain oxygenated groups, especially carbonyls [22, 41, 42]. All the electrochemical treatments completely changed the cyclic voltammetry of this compound. nSPCEs exhibited a very wide peak-to-peak separation, 470 mV, while the activated electrodes showed a peak separation in the order of ~100 mV (save pretreatment 1Na, which provided a peak-to-peak separation of 650 mV). Once again, the higher current capacitances in those treatments using H_2SO_4, particularly for treatments 5S and 7SH, were noteworthy. These results indicate that electrochemical

activation introduces some new oxygenated functional groups, such as carbon-oxygen groups (*vide infra*). To corroborate this assumption and to explore the nature of these functional groups, an XPS analysis was performed.

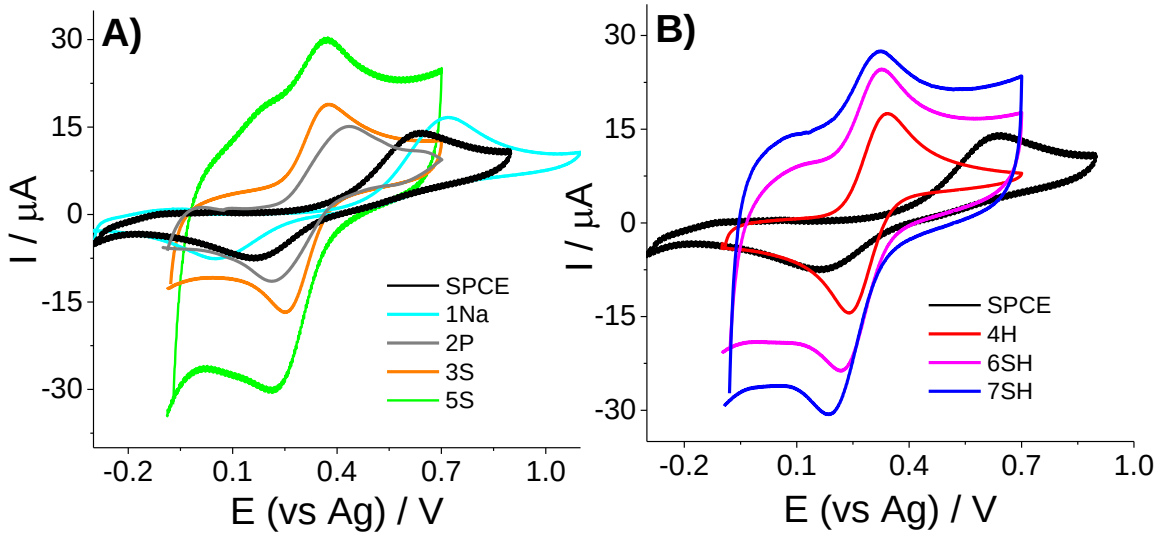

Figure 4. Cyclic voltammetric responses to 1 mM ammonium iron (II) sulfate (in 0.2 M $HClO_4$) using the nSPCE and aSPCEs obtained after different activation pretreatments. Scan rate: 50 mVs^{-1}.

Accordingly, XPS experiments were performed to assess the surface chemistry of the different electrochemically pretreated aSPCEs. The data on the surface atomic concentrations of C and O are shown in Table 4. Generally, the XPS deconvolution of C 1s demonstrates the presence of the main binding energy peaks at 284.6, 285.6, 286.4 and 288.7 eV, which are attributed to the presence of C-C graphitic, C-C aliphatic and C-H, C-O and C-O-C groups, and C=O in carboxyl groups, respectively [43]. The content of C-C graphitic clearly lowered, while O-C=O groups appeared in the activated electrodes, except for treatment 1Na (Figure 5A). The binding energy of 286.4 eV could also be ascribed to the presence of the C-Cl bond, as proven by the presence of the Cl 2p core level depicted in the survey scan (data not shown), which was chemically attributed to the presence of the Cl element used to manufacture carbonaceous inks, as indicated in the previous XPS analysis of SPCEs [44].

Table 4. The XPS results for the untreated SPCEs and electrodes subjected to pretreatments.

Pretreatment	C 1s at %	O 1s at %
None	94.17	5.65
1Na	93.81	6.01
2P	82.84	16.12
3S	78.88	19.67
4H	83.68	14.8
5S	70.91	26.13
6SH	78.00	20.83
7SH	77.86	21.06

The deconvolution of the O 1s spectra for all the electrodes pretreated by the different methodologies is depicted in Figure 5B, where the bands at ca. 532.0 and 533.5 eV are the most representative ones ascribed to the C=O and C-O functional groups (yellow and green bands, respectively) [45]. Furthermore, the presence of O-H in carboxyl for pretreated electrodes 6SH and 7SH is demonstrated (pink bands) (see also the XPS spectra of 3S and 5S compared to 6SH and 7SH, respectively, in Figures 5S and 6S of the Supplementary Material), which could be related to their enhanced electrochemical properties.

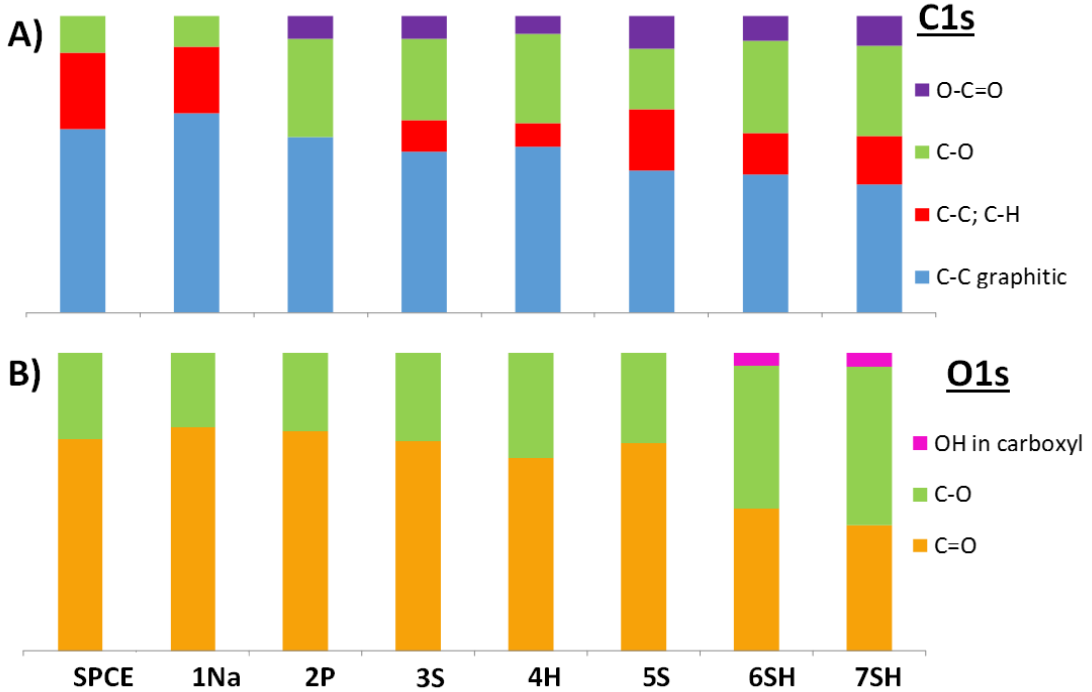

Figure 5. The XPS surface study of the nSPCE and electrodes subjected to the different pretreatments. A) The XPS deconvolution of C 1s. B) The XPS deconvolution of O 1s.

A close inspection of the atomic concentration (at.%) of oxygen, as displayed in Table 4, proved the effect of the oxidizing agent nature on the oxygenated functionalization of SPCEs. The high resolution for the analysis of the O 1s core level showed an oxygen atomic concentration between 14-16 at.% in the electrodes activated by 4H and 2P (compared to the 5-6 at.% for nSPCEs). Moreover, activation by 1Na gave similar at.% values to those depicted by the untreated SPCEs, which agrees with their similar electroanalytical sensitivities (Table 2). The effect of pretreatments 3S, 5S, 6SH and 7SH on the surface chemistry of SPCEs was noteworthy, where the oxygen atomic concentration gave values between 20-26 at.%, which demonstrates the strongest oxidizing conditions of the above solutions. It is worth noting that pretreatments 6SH and 7SH displayed the presence of OH groups in carboxyl functionalization and higher C-O to C=O ratios (Figure 5B), unlike any other pretreatment done in this study.

All these results suggest that high oxygenated atomic content and a high C-O to C=O ratio, as well as the presence of OH groups in carboxyl functionalization, might be correlated with the highest sensitivities for H_2O_2 sensing. One of the possible reasons for that could be ascribed to the contribution of oxygen-containing groups onto the SPCEs surface on the improvement of the wettability, which could promote the diffusion-controlled process and thus enhance the electron transfer rate of SPCEs [46]. This hypothesis is also supported by previous reports in which a favorable electrochemical response towards the direct electron transfer of cytochrome c due to surface carbonyl groups, and to a certain extent carboxylic groups, likely residing at edge plane like – sites/defects of screen-printed graphite electrodes was found [47]. Furthermore, and more recently, improved electrochemical responses towards $K_3[Fe(CN)_6]$ and NADH have also been obtained with SPCEs treated with UV/ozone, mainly attributed to the increase of the number of surface oxygen functional groups [48].

3.3. Electrochemical behavior of aSPCEs 7SH to hydroquinone, acetaminophen and dopamine

Based on the previous results, we selected pretreatment 7SH to obtain improved sensitivity outputs in SPCEs. To extend the applicability of these aSPCEs, the

electrochemical behavior of some model organic compounds of interest was measured by cyclic voltammetry as a proof of concept for the aSPCEs treated by protocol 7SH. These compounds have been chosen as model electroactive species given their widespread use in the chemical and pharmaceutical industries. Acetaminophen is a widespread analgesic and antipyretic oral drug [31]. Hydroquinone is a common environmental pollutant used extensively in multiple industrial processes [32]. Dopamine is an essential neurotransmitter and a clinically valuable diagnostic indicator [33].

Figure 6 shows the cyclic voltammetries obtained for 1 mM acetaminophen, hydroquinone and dopamine using an nSPCE and an aSPCE activated by 7SH. The analytical measurements using aSPCE showed a significant increase in the current intensity of the anodic peak of these compounds, and a shift to less positive potentials. At a scan rate of 50 mVs^{-1}, a lower peak-to-peak separation was observed in aSPCEs (~60, 110 and 130 mV for acetaminophen, hydroquinone and dopamine, respectively) compared to nSPCEs (~400, 450 and 230 mV for acetaminophen, hydroquinone and dopamine, respectively). Therefore, activation process 7SH not only reached enhanced output in the electroanalysis of H_2O_2, but also improved these results of SPCEs to other important biological compounds, which demonstrates its versatility in the electroanalysis field.

Double logarithmic plots of anodic peak currents (Ip_a) *vs.* scan rate before and after activation process 7SH can provide us with information about the kinetic behavior of these compounds on the electrode surface before and after the activation process (Supplementary Material, Figure 7S). Using an nSPCE, a slope of ~0.5 was obtained for the oxidation of acetaminophen, which agrees with the theoretical slope for diffusion controlled processes [49]. However, this slope came close to 1 when an aSPCE (7SH) was used, which is the ideal value for adsorption controlled processes [49]. This result indicates that the changes achieved on the electrode surface after electrochemical pretreatment (*vide supra*) favor the adsorption of acetaminophen molecules on the electrode surface to carry out the electron transfer. However, this does not necessarily mean that adsorption should be the determining step for the electrooxidation of acetaminophen when using aSPCEs. In addition, the Ip_a/Ip_c (anodic peak current intensity/cathodic peak current intensity) ratio deviations from the unity were obtained for acetaminophen, which were more pronounced at the slowest scan rates, regardless of

whether electrodes had been pretreated or not (Figure 8S (A) in Supplementary Material). This behavior should be attributed to complex coupled chemical reactions, in which the semiquinone imine radical product of the oxidation of paracetamol [31] is very likely involved. It is well-known that these radicals readily polymerize to passivate solid electrodes' surfaces [50].

For hydroquinone, the slopes showed a diffusion controlled process for both nSPCE and aSPCE (Figure 7S), with an Ip_a/Ip_c ratio that came close to unity for all the scan rates (Figure 8S). This result well agrees with a more reversible redox cyclic behavior previously reported for this compound [51].

The double logarithmic plots of anodic Ip *versus* the scan rate showed a diffusion controlled process for the oxidation of dopamine, regardless of using nSPCEs or aSPCEs (Figure 7S), and a magnitude of the Ip_a/Ip_c ratio of 3 and 2.5 (Figure 8S), respectively, at the lowest scan rate. This behavior should, once again, be attributed to a chemical coupled reaction, where oxidized species dopamine *o*-quinone undergo intramolecular cyclization to leucodopaminechrome (LDAC) [52]. Only at higher scan rates did the Ip_a/Ip_c ratios approach unity by reducing LDAC formation on the electrode surface.

Finally, even though the evolution pathways of oxidation products are rough irrespectively of employing untreated or treated SPCEs, the use of aSPCEs (7SH pretreatment) markedly enhanced the anodic current intensity for the electrooxidation of acetaminophen, hydroquinone and dopamine, along with greater reversibility of the process, which is most significant in the electroanalysis field.

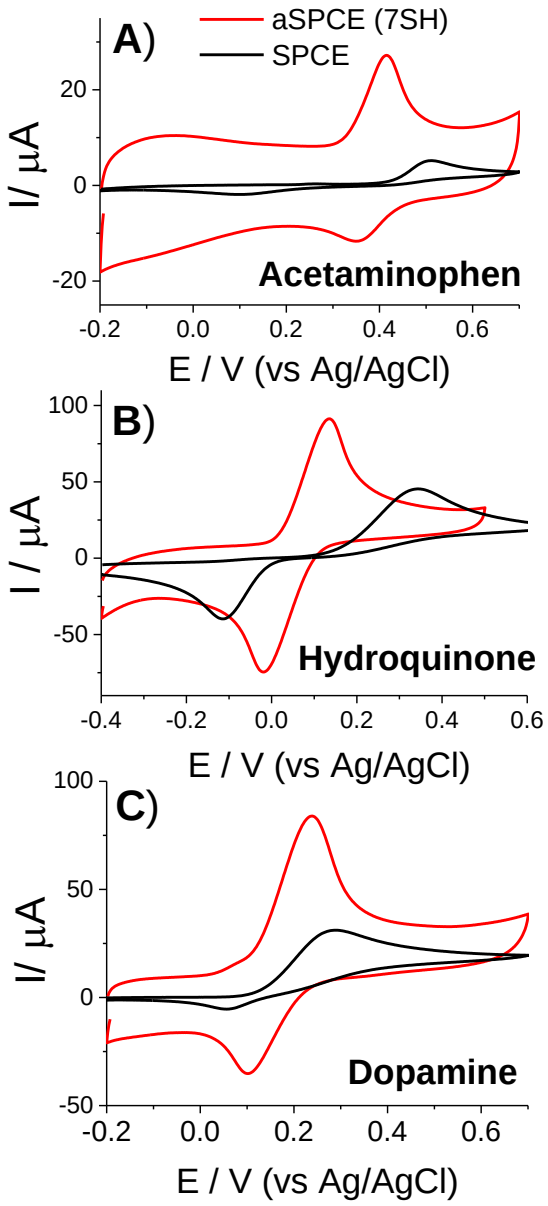

Figure 6. Cyclic voltammetry of 1 mM of some important phenolic compounds using an nSPCE and an aSPCE activated by the 7SH method. Measurements were taken in PB pH 7 at 25ºC. The scan rate was 50 mVs^{-1}.

4. Conclusions

The electrochemical pretreatment of screen-printed carbon electrodes by cyclic voltammetry allowed us to obtain devices with improved electrochemical properties and promising electroanalytical applications. Impedances showed that the activation of SPCEs generally reduced resistance to charge transfer. Nonetheless, the standard Randles equivalent circuit could not explain the behavior observed with activated electrodes 5S and 7SH, which was probably due to the major modification of the surface caused by the most concentrated sulfuric acid. The results indicated that the improvement in electrochemical properties was due mainly to the formation of oxygenated functional groups during the activation process. Furthermore in those cases in which H_2SO_4 was used (3S, 5S, 6SH and 7SH), the increase in the electroactive area and roughness could also contribute to the enhanced electrochemical properties of SPCEs. It was demonstrated, on the other hand, that a pretreatment consisting in two electrochemical steps with diluted H_2SO_4 and H_2O_2, i.e.7SH, was the most effective for the diffusional oxidation of H_2O_2. Protocol 7SH helped to activate electrodes by about 518-fold compared to the unactivated SPCEs, and by 22-fold compared to an SPPtE for the electroanalysis of H_2O_2. This proved a very relevant finding to develop sensitive H_2O_2 sensors based on carbon inks. Furthermore, the aSPCEs submitted to the 7SH activation protocol were very versatile as the electrodes activated by this method show improved electroanalytical outcomes to other important biological compounds (acetaminophen, hydroquinone and dopamine).

FUNDING SOURCE

This work was funded by the Spanish Ministry of Economy and Competitiveness (MINECO, http://www.mineco.gob.es/portal/site/mineco/idi), Projects No. BFU2016-75609-P (AEI/FEDER, UE) and CTQ2016-76231-C2-2-R, and by the Junta de Comunidades de Castilla-La Mancha (Spain), Project No. SBPLY/17/180501/000276/2 (cofunded with FEDER funds, EU). BGM is a post-doctoral research fellow of the Youth Employment Initiative (JCCM, Spain, cofunded with ESF funds, EU). The funders played no role in the study design, data collection and analysis, decision to publish, or preparation of the manuscript.

REFERENCES

[1] F. Arduini, L. Micheli, D. Moscone, G. Palleschi, S. Piermarini, F. Ricci, G. Volpe, Electrochemical biosensors based on nanomodified screen-printed electrodes: Recent applications in clinical analysis, Trac-Trends in Analytical Chemistry 79 (2016) 114-126.

[2] A. Hayat, J.L. Marty, Disposable screen printed electrochemical sensors: tools for environmental monitoring, Sensors 14 (2014) 10432-10453.

[3] Z. Taleat, A. Khoshroo, M. Mazloum-Ardakani, Screen-printed electrodes for biosensing: a review (2008-2013), Microchimica Acta 181 (2014) 865-891.

[4] Z. Chu, J. Peng, W. Jin, Advanced nanomaterial inks for screen-printed chemical sensors, Sensors and Actuators B: Chemical 243 (2017) 919-926.

[5] P.T. Lee, R.G. Compton, Selective electrochemical detection of thiol biomarkers in saliva using multiwalled carbon nanotube screen-printed electrodes, Sensors and Actuators B: Chemical 209 (2015) 983-988.

[6] M. I. González-Sánchez, J. Agrisuelas, E. Valero, R.G. Compton, Measurement of total antioxidant capacity by electrogenerated iodine at disposable screen printed electrodes, Electroanalysis 29 (2017) 1316-1323.

[7] J.-M. Jian, L. Fu, J. Ji, L. Lin, X. Guo, T.-L. Ren, Electrochemically reduced graphene oxide/gold nanoparticles composite modified screen-printed carbon electrode for effective electrocatalytic analysis of nitrite in foods, Sensors and Actuators B: Chemical 262 (2018) 125-136.

[8] K.L. Westmacott, A. Crew, O. Doran, J.P. Hart, A novel electroanalytical approach to the measurement of B vitamins in food supplements based on screen-printed carbon sensors, Talanta 181 (2018) 13-18.

[9] D. Martin-Yerga, E. Costa Rama, A. Costa Garcia, Electrochemical study and determination of electroactive species with screen-printed electrodes, Journal of Chemical Education 93 (2016) 1270-1276.

[10] M. I. González Sánchez, B. Gómez Monedero, J. Agrisuelas, E. Valero, Recycling metals from spent screen-printed electrodes while learning the fundamentals of electrochemical sensing, Journal of Chemical Education 95 (2018) 847-851.

[11] M. Tudorache, C. Bala, Biosensors based on screen-printing technology, and their applications in environmental and food analysis, Analytical and Bioanalytical Chemistry 388 (2007) 565-578.

[12] S. Kubendhiran, S. Sakthinathan, S.M. Chen, C.M. Lee, B.S. Lou, P. Sireesha, C.C. Su, Electrochemically activated screen printed carbon electrode decorated with nickel nanoparticles for the detection of glucose in human serum and human urine sample, International Journal of Electrochemical Science 11 (2016) 7934-7946.

[13] D. Pan, S.Z. Rong, G.T. Zhang, Y.N. Zhang, Q. Zhou, F.H. Liu, M.J. Li, D. Chang, H.Z. Pan, Amperometric determination of dopamine using activated screen-printed carbon electrodes, Electrochemistry 83 (2015) 725-729.

[14] J. Wang, M. Pedrero, H. Sakslund, O. Hammerich, J. Pingarrón, Electrochemical activation of screen-printed carbon strips, Analyst 121 (1996) 345-350.

[15] K. Stulik, Activation of solid electrodes, Electroanalysis 4 (1992) 829-834.

[16] C. Churinsky, C. Grgicak, The effect of repeated activation on screen-printed carbon electrode cards, Student Posters (General) - 225th ECS Meeting 61 (2014) 1-8.

[17] K. Shi, K.K. Shiu, Determination of uric acid at electrochemically activated glassy carbon electrode, Electroanalysis 13 (2001) 1319-1325.

[18] Screen-Printed electrode information. Carbon and ceramic electrode information, Pine Research, 2016.https://www.pineresearch.com/shop/wp-content/uploads/sites/2/2016/10/DRP10036-Screen-Printed-Electrodes-Overview-REV001.pdf.

[19] R. Gusmao, V. López-Puente, I. Pastoriza-Santos, J. Pérez-Juste, M.F. Proenca, F. Bento, D. Geraldo, M.C. Paiva, E. González-Romero, Enhanced electrochemical sensing of polyphenols by an oxygen-mediated surface, RSC Advances 5 (2015) 5024-5031.

[20] Y.L. Su, C.Y. Tai, J.M. Zen, A simple method to tune up screen-printed carbon electrodes applicable to the design of disposable electrochemical sensors, Electroanalysis 25 (2013) 2539-2546.

[21] S.C. Wang, K.S. Chang, C.J. Yuan, Enhancement of electrochemical properties of screen-printed carbon electrodes by oxygen plasma treatment, Electrochimica Acta 54 (2009) 4937-4943.

[22] L.R. Cumba, C.W. Foster, D.A.C. Brownson, J.P. Smith, J. Iniesta, B. Thakur, D.R. do Carmo, C.E. Banks, Can the mechanical activation (polishing) of screen-printed electrodes enhance their electroanalytical response?, Analyst 141 (2016) 2791-2799.

[23] G.D. Pierini, C.W. Foster, R.-N.S. J., H. Fernández, C.E. Banks, A facile electrochemical intercalation and microwave assisted exfoliation methodology applied to screen-printed electrochemical-based sensing platforms to impart improved electroanalytical outputs, Analyst, 143 (2018) 3360-3365.

[24] G. Cui, J.H. Yoo, J.S. Lee, J. Yoo, J.H. Uhm, G.S. Cha, H. Nam, Effect of pre-treatment on the surface and electrochemical properties of screen-printed carbon paste electrodes, Analyst 126 (2001) 1399-1403.

[25] R.O. Kadara, N. Jenkinson, C.E. Banks, Screen printed recessed microelectrode arrays, Sensors and Actuators B-Chemical 142 (2009) 342-346.

[26] P. Fanjul-Bolado, D. Hernández-Santos, P.J. Lamas-Ardisana, A. Martín-Pernia, A. Costa-García, Electrochemical characterization of screen-printed and conventional carbon paste electrodes, Electrochimica Acta 53 (2008) 3635-3642.

[27] D.D. Gornall, S.D. Collyer, S.P.J. Higson, Investigations into the use of screen-printed carbon electrodes as templates for electrochemical sensors and sonochemically fabricated microelectrode arrays, Sensors and Actuators B: Chemical 141 (2009) 581-591.

[28] M.I. González Sánchez, B. Gómez Monedero, J. Agrisuelas, J. Iniesta, E. Valero, Highly activated screen-printed carbon electrode by electrochemical treatment with hydrogen peroxide, Electrochemistry Communications 91 (2018) 36-40.

[29] W. Chen, S. Cai, Q.Q. Ren, W. Wen, Y.D. Zhao, Recent advances in electrochemical sensing for hydrogen peroxide: a review, Analyst 137 (2012) 49-58.

[30] Y. Guangxia, W. Weixiang, P. Xiaoqi, Z. Qiang, W. Xiaoyun, L. Qing, High sensitive and selective sensing of hydrogen peroxide released from pheocromocytoma

cells based on Pt-Au bimetallic nanoparticles electrodeposited on reduced graphene sheets, Sensors 15 (2015) 2709-2722.

[31] M.I. González-Sánchez, M.C. Manjabacas, F. García-Carmona, E. Valero, Mechanism of Acetaminophen Oxidation by the Peroxidase-like Activity of Methemoglobin, Chemical Research in Toxicology (2009) 1841-1850.

[32] X. Niu, L. Yan, X. Li, Z. Wen, J. Yu, A. Hu, L. Dong, Z. Shi, W. Sun, An electrochemical hydroquinone sensor with nitrogen-doped graphene modified electrode, International Journal of Electrochemical Science 11 (2016) 7139-7149.

[33] W. Al-Graiti, Z. Yue, J. Foroughi, X.-F. Huang, G. Wallace, R. Baughman, J. Chen, Probe sensor using nanostructured multi-walled carbon nanotube for selective and sensitive detection of dopamine, Sensors 17 (2017) 884.

[34] Y.J. Wang, J.G. Limon-Petersen, R.G. Compton, Measurement of the diffusion coefficients of $Ru(NH_3)_6^{3+}$ and $Ru(NH_3)_6^{2+}$in aqueous solution using microelectrode double potential step chronoamperometry, Journal of Electroanalytical Chemistry 652 (2011) 13-17.

[35] A.G.M. Ferrari, C.W. Foster, P.J. Kelly, D.A.C. Brownson, C.E. Banks, Determination of the electrochemical area of screen-printed electrochemical sensing platforms, Biosensors-Basel 8 (2018) 53.

[36] A.S. Bondarenko, G.A. Ragoisha, Inverse problem in potentiodynamic electrochemical impeadance, in: Alexey L. Pomerantsev (Ed.), Nova Science Publishers, Prog. Chemom. Res, 2005.

[37] M.I. González-Sánchez, L. González-Maciá, M.T. Pérez-Prior, E. Valero, J. Hancock, A.J. Killard, Electrochemical detection of extracellular hydrogen peroxide in Arabidopsis thaliana: a real-time marker of oxidative stress, Plant Cell and Environment 36 (2013) 869-878.

[38] J. Agrisuelas, M.I. González-Sánchez, E. Valero, Hydrogen peroxide sensor based on *in situ* grown Pt nanoparticles from waste screen-printed electrodes, Sensors and Actuators B-Chemical 249 (2017) 499-505.

[39] M. Zhu, N. Li, J. Ye, Sensitive and selective sensing of hydrogen peroxide with iron-tetrasulfophthalocyanine-graphene-nafion modified screen-printed electrode, Electroanalysis 24 (2012) 1212-1219.

[40] M.H. Martin, A. Lasia, Influence of experimental factors on the constant phase element behavior of Pt electrodes, Electrochimica Acta 56 (2011) 8058-8068.

[41] P.H. Chen, R.L. McCreery, Control of electron transfer kinetics at glassy carbon electrodes by specific surface modification, Analytical Chemistry 68 (1996) 3958-3965.

[42] M.R. Kagan, R.L. McCreery, Quantitative surface Raman-spectroscopy of physisorbed monolayers on glassy-carbon, Langmuir 11 (1995) 4041-4047.

[43] E. Mazzotta, S. Rella, A. Turco, C. Malitesta, XPS in development of chemical sensors, RSC Advances 5 (2015) 83164-83186.

[44] F.E. Galdino, J.P. Smith, S.I. Kwamou, D.K. Kampouris, J. Iniesta, G.C. Smith, J.A. Bonacin, C.E. Banks, Graphite screen-printed electrodes applied for the accurate and reagentless sensing of pH, Analytical Chemistry 87 (2015) 11666-11672.

[45] L. Bai, S. Qiao, Y. Fang, J.G. Tian, J. McLeod, Y.L. Song, H. Huang, Y. Liu, Z.H. Kang, Third-order nonlinear optical properties of carboxyl group dominant carbon nanodots, Journal of Materials Chemistry C 4 (2016) 8490-8495.

[46] K.J. Kim, S.W. Lee, T. Yim, J.G. Kim, J.W. Choi, J.H. Kim, M.S. Park, Y.J. Kim, A new strategy for integrating abundant oxygen functional groups into carbon felt electrode for vanadium redox flow batteries, Scientific Reports 4 (2014) 6906-6911.

[47] M. Gómez-Mingot, J. Iniesta, V. Montiel, R.O. Kadara, C.E. Banks, Screen printed graphite macroelectrodes for the direct electron transfer of cytochrome c, Analyst 136 (2011) 2146-2150.

[48] J. Wang, Z. Xu, M. Zhang, J. Liu, H. Zou, L. Wang, Improvement of electrochemical performance of screen-printed carbon electrodes by UV/ozone modification, Talanta 192 (2019) 40-45.

[49] A.J. Bard, L.R. Faulkner, Electrochemical Methods: Fundamentals and Applications, Second Edition ed, 2004.

[50] N. Karikalan, R. Karthik, S.M. Chen, M. Velmurugan, C. Karuppiah, Electrochemical properties of the acetaminophen on the screen printed carbon electrode towards the high performance practical sensor applications, Journal of Colloid and Interface Science 483 (2016) 109-117.

[51] B.R. Eggins, J.Q. Chambers, Electrochemical oxidation of hydroquinone in acetonitrile, Journal of the Chemical Society D-Chemical Communications 5 (1969) 232-233.

[52] D.C.S. Tse, R.L. McCreery, R.N. Adams, Potential oxidative pathways of brain catecholamines, Journal of Medicinal Chemistry 19 (1976) 37-40.